Code functions for pseudo-random phase encoding (temptative title)

Claudio Guerra and Biondo Biondi

ABSTRACT

The recently introduced prestack exploding reflector modeling aims to model a small dataset comprised by areal shots, while keeping the correct kinematics to be used in iterations of migration velocity analysis. To achieve this goal, the modeled areal data must be combined into sets. By randomly phase encoding the modeling experiments, crosstalk can be attenuated during migration. Here, we exploit the application of phase functions from Gold codes commonly used in wireless communication, radar and medical imaging communities to phase encode data to be migrated. We also introduce a method to compute random phase functions by solving an optimization problem ... (more still to come)

INTRODUCTION

Recently, Biondi (2006, 2007) introduced the concept of the prestack exploding reflector modeling. This method synthesizes source and receiver wavefields along the entire survey at the surface, in the form of areal data, starting from a prestack migrated image cube represented by subsurface-offset domain common-image gathers (SODCIGs). For migration velocity analysis, the aim is to generate a considerably smaller dataset than the one used in the initial migration while maintaining the necessary kinematic information

Conceptually, the synthesized areal data are computed by upward propagating source and receiver wavefields, using as initial condition a subsurface-offset domain common image gather (SODCIG). To decrease the number of experiments to migrate, we take advantage of the linearity of the wave propagation to combine several experiments into a set of composite records. Combining several experiments, though, gives rise to crosstalk during imaging (Biondi, 2006; Guerra and Biondi, 2008). Guerra and Biondi (2008) use pseudo-random phase encoding (Romero et al., 2000) during the modeling step to attenuate crosstalk. For conciseness reason, from now on we use the term random instead of pseudo-random,

In the exploration geophysics community, are employed pseudo-random codes which auto-correlation and cross-correlation functions have no special property. The peak to side lobe ratio of the auto-correlation function has a high value, however presents random amplitudes at lags different from zero. The cross-correlation function is random with small amplitudes when compared to the peak of the auto-correlation. Herein this code is called conventional random code.

However, in wireless communication, specially for systems which use Code Division Multiple Access (CDMA), different pseudo-random codes have been widely used (Shi and Schelgel, 2003). Medical imaging (Gran, 2005) and radar communities (Levanon and Mozeson, 2004) also exploit the statistical properties of these pseudo-random codes for bandwidth and signal-to-noise ratio increase and pulse compression. These codes are binary sequences and have unique auto-correlation and cross-correlations properties which make them more suitable to achieve the above mentioned objectives with minimal cross-talk. Examples of binary pseudo-random codes used by these communities are Golay (Golay, 1961; Tseng, 1972), Kasami (Kasami, 1966) and Gold codes (Gold, 1967). Here, we exploit the properties of the Gold codes to encode seismic data.

We introduce a novel method to compute phase functions by solving an optimization problem ...

In the next section we give a brief description of the prestack exploding reflector modeling. Then we discuss how to compute the Gold codes and the optimized random phase functions. We illustrate the application of each phase encoding scheme by migrating groups of four neighboring encoded shots of Marmousi model and phase encoded areal data synthesized by prestack exploding reflector modeling.

PRESTACK EXPLODING REFLECTOR MODELING

Starting from a prestack image obtained by means of wave-equation migration, areal source and receiver wavefields are modeled at the surface by:

$$\begin{aligned} S(x,\omega) &= G(z_\xi, x_\xi - h_\xi; x, z=0, \omega) * I_s(z_\xi, x_\xi, h_\xi), \\ R(x,\omega) &= G(z_\xi, x_\xi + h_\xi; x, z=0, \omega) * I_r(z_\xi, x_\xi, h_\xi), \end{aligned} \tag{1}$$

where $S(x,\omega)$ is the source wavefield at $z=0$; $R(x,\omega)$ is the receiver wavefield at $z=0$; $I_s(z_\xi, x_\xi, h_\xi)$ and $I_r(z_\xi, x_\xi, h_\xi)$ are the prestack images used as initial condition for the source and receiver wavefield extrapolation, respectively, at a selected position, x_ξ,; $G(z_\xi, x_\xi \pm h_\xi; x, z=0, \omega)$ represents the operator which extrapolates the wavefields from the subsurface to the surface; h_ξ is the subsurface offset; z_ξ is depth; ω is the temporal frequency and x is the spatial coordinate in the data space coinciding with x_ξ. The prestack images used as initial condition for the source and receiver wavefield extrapolation are supposed to be dip-independent gathers computed by changing the dip along the offset direction according to the apparent geological dip (Biondi, 2007). Here we use one-way extrapolators for both modeling and migration of the areal data.

By combining sets of individual modeling experiments into the same areal data, the amount of input data to migration can be significantly decreased. We achieve this by regularly selecting individual experiments and adding them up into their set, after being upward propagated, according to:

$$\begin{aligned}\widetilde{S}_n(x,\omega) &= \sum_{n=1}^{k}\sum_{i=n,k,N} S_i(x,\omega),\\ \widetilde{R}_n(x,\omega) &= \sum_{n=1}^{k}\sum_{i=n,k,N} R_i(x,\omega),\end{aligned} \tag{2}$$

where $\widetilde{S}_n(x,\omega)$ and $\widetilde{R}_n(x,\omega)$ contains $k-$sets of summed areal sources and areal receivers, respectively; N is the number of SODCIGs. Every other k areal data are selected to compose one set. Pairs of $\widetilde{S}_k(x,\omega)$ and $\widetilde{R}_k(x,\omega)$ are to be used as the areal source function and the areal receiver wavefield, respectively, in areal shot migration.

Migration of the combined areal data produces an image by cross-correlating the combined areal source and receiver wavefields,

$$\widetilde{I}_m(z_\xi,x_\xi,h_\xi)=\sum_{\omega}\widetilde{S_m}^{\star}(z_\xi,x_\xi-h_\xi,\omega)\widetilde{R}_m(z_\xi,x_\xi+h_\xi,\omega), \tag{3}$$

where * represents complex conjugation. If $\widetilde{S_m}(x,\omega)$ and $\widetilde{R_m}(x,\omega)$ in equation 2 are comprised by two summed areal shots, the image $\widetilde{I_m}(z_\xi,x_\xi,h_\xi)$ will be given by:

$$\begin{aligned}\widetilde{I_m}(z_\xi,x_\xi,h_\xi) = {} & I_1(z_\xi,x_\xi,h_\xi)+I_2(z_\xi,x_\xi,h_\xi)+\\ & \sum_{\omega} S_1^{\star}(z_\xi,x_\xi-h_\xi,\omega)R_2(z_\xi,x_\xi+h_\xi,\omega)+\\ & \sum_{\omega} S_2^{\star}(z_\xi,x_\xi-h_\xi,\omega)R_1(z_\xi,x_\xi+h_\xi,\omega).\end{aligned} \tag{4}$$

In equation 4, the last two summation terms represent the crosstalk.

Guerra and Biondi (2008) show that in the prestack exploding reflector method the crosstalk have two distinct origins. The crosstalk which is prominent in the zero-subsurface offset section is due to the cross-correlation of events in the source wavefield with that in the receiver wavefields modeled by the same SODCIG, which herein we call type-1. Crosstalk in non-zero subsurface offsets is related to cross-correlation of events in the source wavefields with that in the receiver wavefields modeled by different SODCIGs, which herein we call type-2.

Guerra and Biondi (2008) introduce strategies to attenuate the crosstalk and show that migration of areal data, (x,z,ω)-randomly phase encoded during the modeling, disperses the crosstalk energy throughout the image as a pseudo-random background noise. By adding the migration of more realizations of random phase encoded areal data attenuates the speckled noise.

PSEUDO-RANDOM CODES

Gold codes

Before describing Gold codes it is useful to define maximum length sequences.

Linear feedback shift registers (LFSR) are called state machines whose main operations are:

- compute the input bit according to the tap sequence;
- shift the bit pattern;
- register the output bit; and
- insert the bit computed in 1 into the input bit position.

Maximum length sequences (m-sequences) are composed by the output bits of a LFSR. They are, by definition, the largest codes that can be generated by a LFSR for a given tap sequence.

The tap sequence defines which bits in the current state will be combined to determine the input bit for the next state, generally using module-2 addition (*exclusive or*). Tap sequences can be represented by irreducible polynomials over **GF**(2) (*Galois Field* of order 2) – polynomials with coefficients either 0 or 1 which cannot be represented as the product of two or more polynomials. For example, x^2+1 is not irreducible over **GF**(2) because it can be factored into $x+1$:

$$(x+1)(x+1) = x^2+2x+1 \equiv x^2+1. \tag{5}$$

Considering an irreducible polynomial, the corresponding tap sequence is given by the exponents whose polynomial coefficients are 1 (Dinan and Jabbari, 1998). M-sequences are binary pseudo-random sequences of (p^n-1)–length, where n is the number of elements of the tap sequence and $p = 2, 3$ *or* 5.

The autocorrelation function of an m-sequence, $\Phi_{mls}(k)$, is given by

$$\Phi_{mls}(k) = \begin{cases} p^n - 1 & \text{for} \quad k = 0, \\ -1 & \text{for} \quad k \neq 0 \end{cases} \tag{6}$$

where k is the lag of correlation. In spite of the good autocorrelation properties, m-sequences, in general, are not immune to cross-correlation problems, and they may have large and unpredictable cross-correlation values. However, the so-called preferred pairs of m-sequences have cross-correlation functions which might assume the predicted values, -1, $-1+p$, and $-1-p$, where $p = 2^{(n+1)/2}$ for n odd or $p = 2^{(n+2)/2}$ for n even. Given a (2^n-1)–length m-sequence, $a(k)$, with $(n,4) \neq 0$, its preferred pair is the result of decimation computed by applying on $a(k)$ a circular shift of q samples, where $q = 2k+1$ and $gcd\{k,n\} = 1$. Figure 1 shows the autocorrelation of an m-sequence on the top and the its cross-correlation with its preferred pair computed with $k = 5$.

The number of possible preferred pairs of m-sequences is limited, when compared to the requirements of practical applications of wireless communication. However, preferred-pairs of m-sequences can be used to generate Gold codes (Dinan and Jabbari, 1998).

In CDMA, Gold codes are used as chipping sequences that allow several callers to use the same frequency, resulting in less interference and better utilization of the available bandwidth. As originally proposed by Gold (1967), Gold codes can be computed by module-2

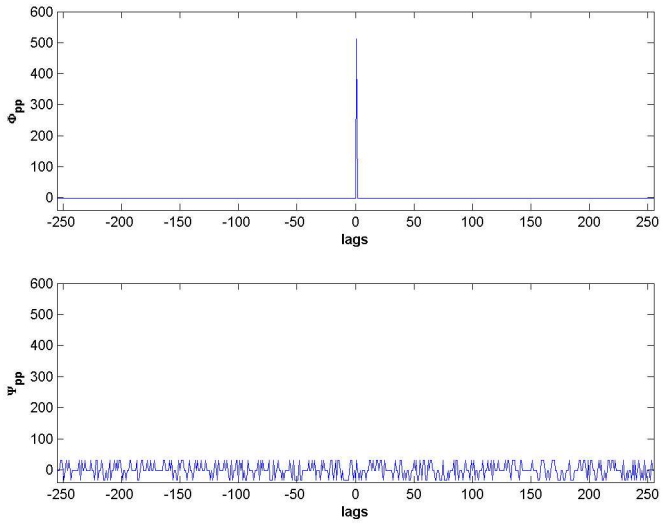

Figure 1: Correlation functions of preferred pairs of m-sequences. On the top: autocorrelation of an m-sequence. On the bottom: cross-correlation of a preferred-pair of m-sequence. prefpairs [NR]

addition (*exclusive or*) of circularly shifted preferred pairs of m-sequences of length $2^n - 1$. The autocorrelation function of a Gold sequence, $\Phi_{gc}(k)$, is given by:

$$\Phi_{gc}(k) = \begin{cases} 2^n - 1 & \text{for} \quad k = 0, \\ -1 & \text{for} \quad k \neq 0. \end{cases} \tag{7}$$

More interestingly, the two valued cross-correlation function of Gold sequences, $\Psi_{gc}(k)$, is given by

$$\Psi_{gc}(k) = \begin{cases} \pm(2^n - 1) & \text{for} \quad k = \lambda, \\ -1 & \text{for} \quad k \neq \lambda. \end{cases} \tag{8}$$

where the correlation lag λ is given by the difference between the number of circular shifts applied to the m-sequence to compute the Gold code.

Figure 2 illustrates the correlation properties of the Gold codes. The top part shows the autocorrelation of the Gold code generated with one circular shift of the preferred-pair of m-sequence. The bottom part shows the cross-correlation of the Gold code generated with one circular shift of the preferred-pair of m-sequence with that generated with 84 circular shifts. The peak of the cross-correlation occurs at lag 84. The Gold codes have 255 samples.

Optimized random codes

...

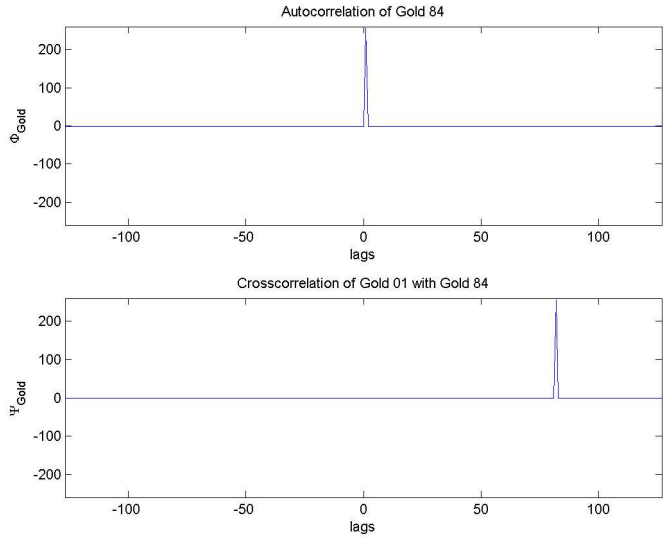

Figure 2: Correlation functions of Gold codes. On the top, autocorrelation of Gold code generated with one circular shift of the preferred-pair of m-sequence. On the bottom, cross-correlation of the Gold code generated with one circular shift of the preferred-pair of m-sequence with that generated with 84 circular shifts. The peak of the cross-correlation occurs at lag 84. gold184 [NR]

EXAMPLES

We show two examples of using Gold codes in phase encoding. In the first one, we migrate encoded shots of Marmousi data using Gold codes and conventional random-phase codes. In the second example we use Gold codes to encode modeling experiments in the prestack exploding reflector method applied to a simple model of two intersecting reflectors embeded in constant velocity medium. Migration and modeling were performed using the phase-shift plus interpolation (PSPI) technique ofGazdag and Sguazzero (1984).

Marmousi

Marmousi data are composed of 240 shots and 256 frequencies. In all migrations we used the correct velocity and computed 33 subsurface offsets ranging from -400 m to 400 m. The reference velocities were computed by the Lloyd's method (Clapp, 2004). For comparison, Figure 3 shows the shot-profile migration of non-encoded shots using a migration aperture of 7500 m. The left panel corresponds to the zero-subsurface offset section and the right panel is the subsurface offset gather taken at the x-position indicated by the vertical line in the zero-subsurface offset section.

For the random phase encoding examples, we migrated groups of four encoded shots. Data were encoded in both frequency and shot dimensions using conventional random codes and

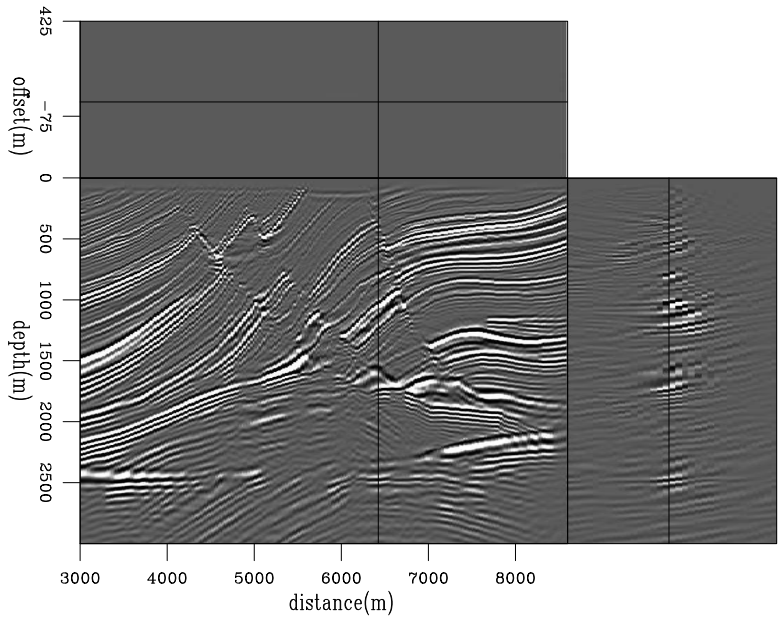

Figure 3: Shot profile migration using PSPI of Marmousi. Marmsp [CR]

Gold codes. Figure 4 shows the migration of groups of four conventional randomly encoded shots. Figure 5 shows the migration of groups of four encoded shots using Gold codes. Figure 6 shows the migration of the encoded data using the optimized codes.

The difference sections between the shot profile migration and the conventional random phase encoding migration, Gold code phase encoding migration and optimized phase encoding migration are shown in Figures 7, 8 and 9, respectively. These figures are displayed with the same clip of the migrated images. Again, no obvious advantage of one encoding method over the other can be highlighted.

Prestack exploding reflector modeling of intersecting reflectors

Figure 10 shows the areal shot migration of data generated by the prestack exploding reflector modeling with no phase encoding applied. The SODCIG's input to modeling were computed by shot-profile migration with the correct velocity. The combined areal data are comprised of modeling experiments separated by every ten SODCIG's. The number of subsurface offsets is 33. For the areal shot migration, the zero-subsurface offset section, on the left, shows strong type-1 crosstalk as a reflector with an intermediate dip. Type-2 crosstalk is present in the SODCIG, on the right. Our objective by phase encoding the modeling experiments is to achieve a satisfactory crosstalk attenuation.

We use conventional random codes and Gold codes to encode the modeling experiments. Figure 11 shows the areal shot migration of four realizations of conventional randomly encoded data and Figure 12 presents the areal shot migration of four realizations of Gold encoded data. In both results the crosstalk has been largely attenuated, being dispersed throughout the

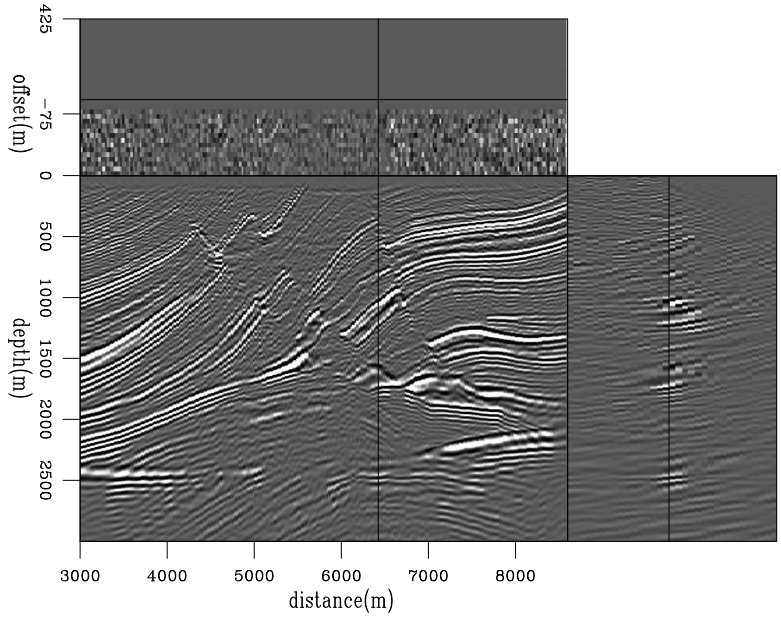

Figure 4: Migration of randomly phase encoded groups of four neighboring shots using conventional random codes. Marmr4 [CR]

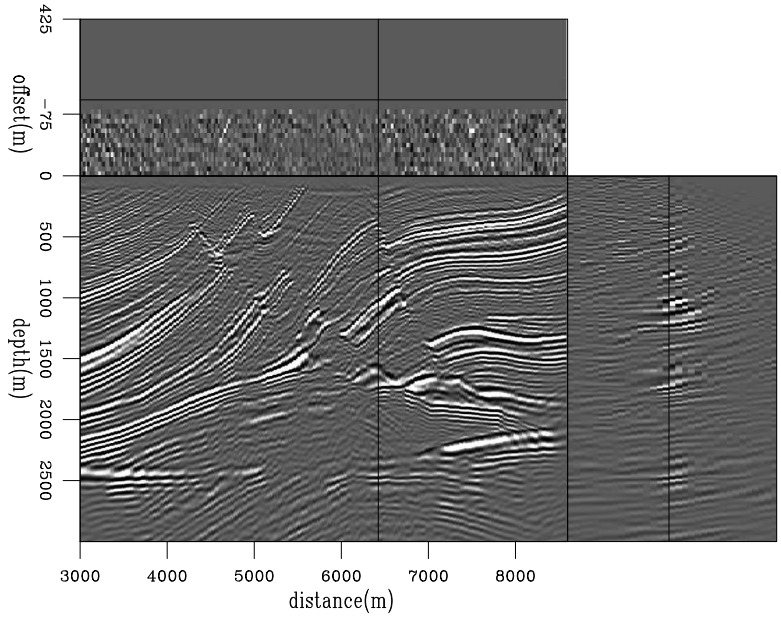

Figure 5: Migration of randomly phase encoded groups of four neighboring shots using Gold codes. Marmg4 [CR]

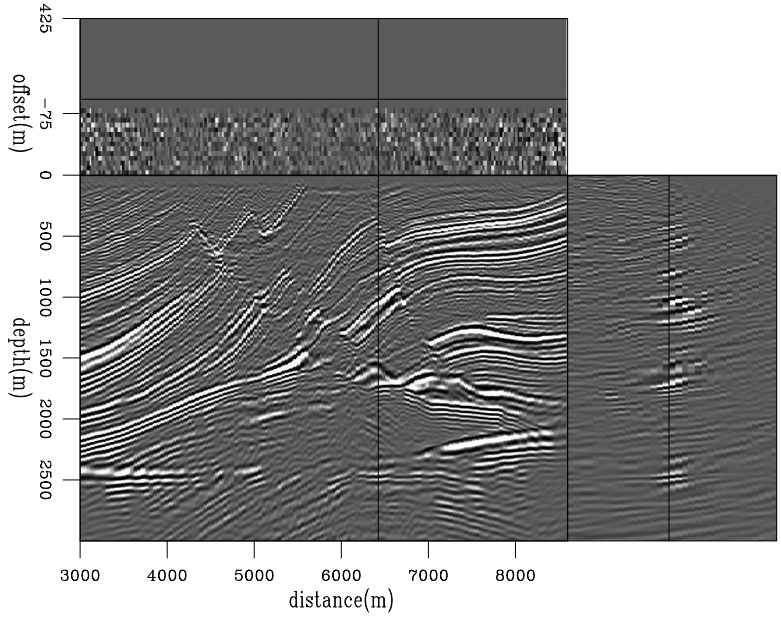

Figure 6: Migration of randomly phase encoded groups of four neighboring shots using phases from simulated annealing. Marmsa [CR]

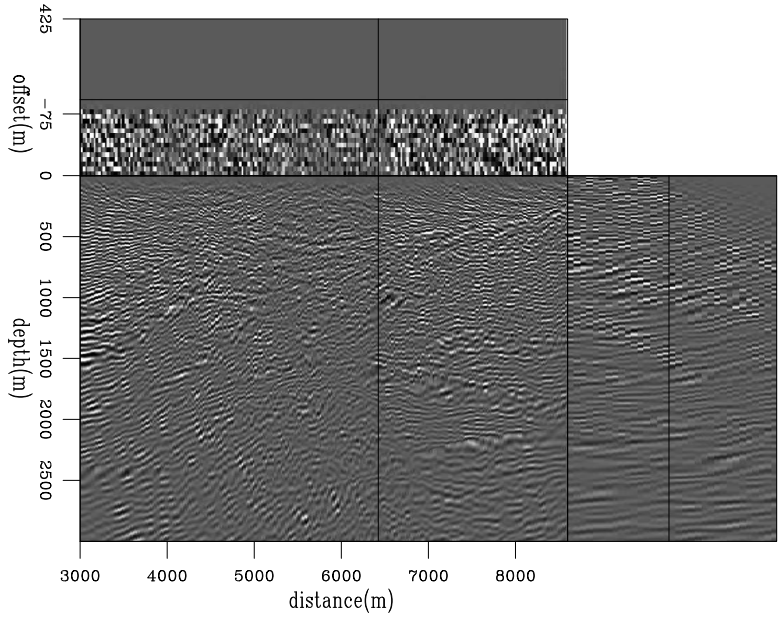

Figure 7: Difference between shot profile migration and migration of randomly phase encoded groups of four neighboring shots using conventional random codes. Marmdifr4 [CR]

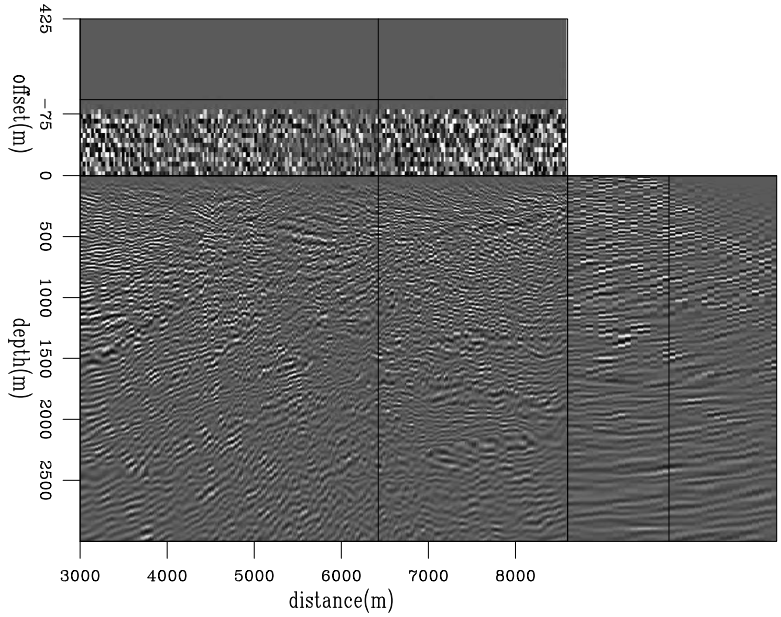

Figure 8: Difference between shot profile migration and migration of randomly phase encoded groups of four neighboring shots using Gold codes. Marmdifg4 [CR]

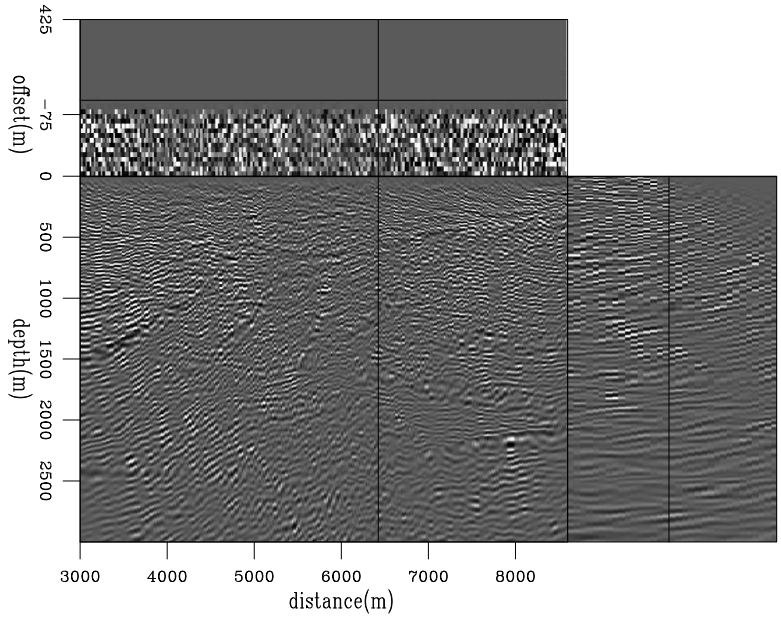

Figure 9: Difference between shot profile migration and migration of randomly phase encoded groups of four neighboring shots using phases from simulated annealing. Marmdifsa [CR]

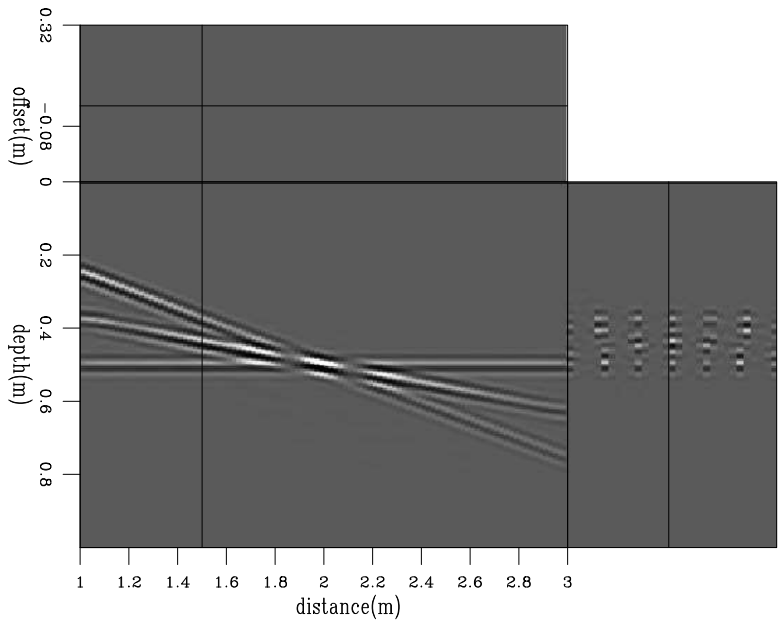

Figure 10: Areal shot migration of data generated by the prestack exploding reflector modeling with no phase encoding applied. Perm0 [CR]

image. Similarly to what we observed in the Marmousi examples, there are no conspicuous advantage of one encoding method over the other.

DISCUSSION

Because Gold codes have length of $2^n - 1$, its use in phase encoding imposes some constraints in data dimensions which must be $(2^n - 1)$–length in the encoded direction. As its results are equivalent to those obtained with conventional or optimized random codes, there is no advantage of using Gold codes since no dimension constraints exist for these two random codes.

The fact that phase encoding migration results are similar can be explained by the fact that, considering a uniform distribution for the random phases, the crosstalk should be reduced by a factor of $1/\sqrt{n_\omega}$ for (x,ω)–encoded shots and $1/\sqrt{n_\omega n_z}$ for (x,z,ω)–encoded prestack exploding reflector modeling experiments.

More still to come ...

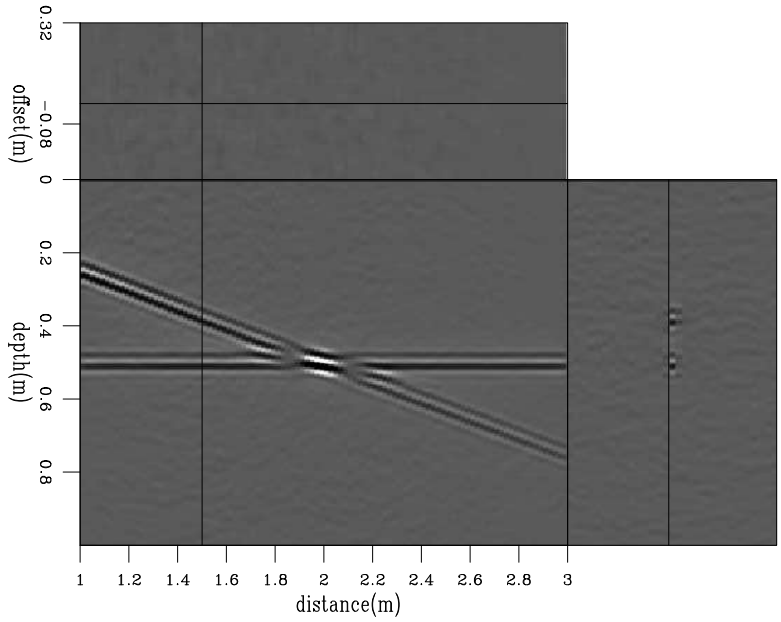

Figure 11: Areal shot migration of data generated by the prestack exploding reflector modeling using conventional random phase encoded areal data. conv4r [CR]

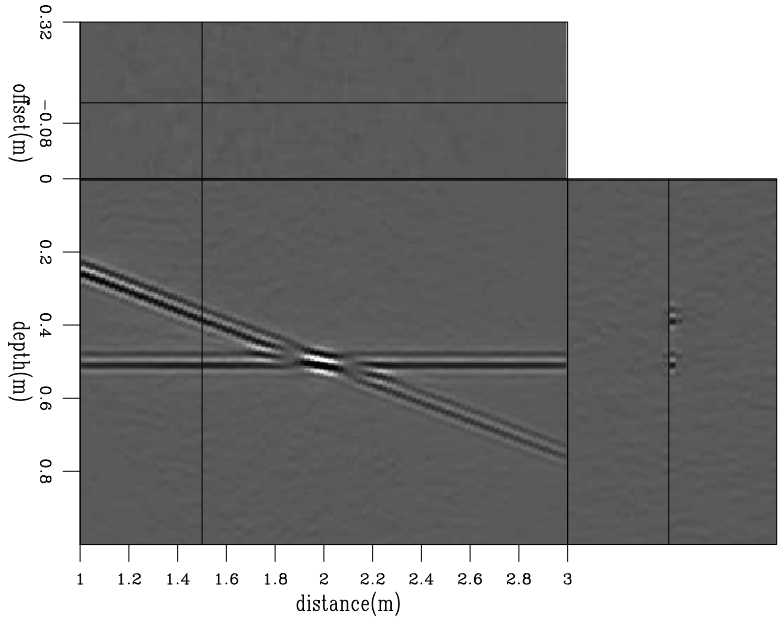

Figure 12: Areal shot migration of data generated by the prestack exploding reflector modeling using Gold codes to encode the areal data. gold4r [CR]

REFERENCES

Biondi, B., 2006, Prestack exploding-reflectors modeling for migration velocity analyis: SEP–**124**, 45–60.

Biondi, B., 2007, Prestack modeling of image events for migration velocity analysis: SEP-131, pages 101–118.

Clapp, R. G., 2004, Reference velocity selection by a generalized lloyd method: SEG Technical Program Expanded Abstracts, **23**, no. 1, 981–984.

Dinan, E. and B. Jabbari, 1998, Spreading codes for direct sequence CDMA and wideband CDMA cellular networks: IEEE Communications Magazine, **36**, no. 9, 48–54.

Gazdag, J. and P. Sguazzero, 1984, Migration of seismic data by phase shift plus interpolation: Geophysics, **49**, no. 2, 124–131.

Golay, M., 1961, Complementary sequences: IRE Trans. on Info.Theory, **IT-7**, 82–87.

Gold, R., 1967, Optimal binary sequences for spread spectrum multiplexing: IEEE Transactions on Information Theory, **14**, no. 4, 619–621.

Gran, F., 2005, Spatio-temporal encoding in medical ultrasound imaging: Ph.D. thesis, Technical University of Denmark.

Guerra, C. and B. Biondi, 2008, Prestack exploding reflector modeling: The crosstalk problem: SEP-134, pages 79–91.

Kasami, T., Weight distribution formula for some class of cyclic codes:, Technical Report R-285, 1966.

Levanon, N. and E. Mozeson, 2004, Radar Signals: John Wiley & Sons.

Romero, L., D. Ghiglia, C. Ober, and S. Morton, 2000, Phase encoding of shot records in prestack migration: Geophysics, **65**, 426–436.

Shi, Z. and C. Schelgel, 2003, Spreading code construction for CDMA: IEEE Communications letters, **1**, no. 7, 4–6.

Tseng, C., 1972, Complementary sets of sequences: IEEE Trans. on Info.Theory, **IT-18**, no. 5, 644–652.